Relation between Wigner energy and proton-neutron pairing

I. Bentley[1,2] and S. Frauendorf[1]

[1]*Department of Physics, University of Notre Dame, Notre Dame, Indiana 46556, USA*
[2]*Department of Chemistry and Physics, Saint Mary's College, Notre Dame, Indiana 46556, USA*

The linear term proportional to $|N - Z|$ in the nuclear symmetry energy (Wigner energy) is obtained in a model that uses isovector pairing on single-particle levels from a deformed potential combined with a $\vec{T}^2$ interaction. The pairing correlations are calculated by numerical diagonalization of the pairing Hamiltonian acting on the six or seven levels nearest the $N = Z$ Fermi surface. The experimental binding energies of nuclei with $N \approx Z$ are well reproduced. The Wigner energy emerges as a consequence of restoring isospin symmetry. We have found the Wigner energy to be insensitive to the presence of moderate isoscalar pair correlations.

I. INTRODUCTION

The nuclear ground-state energy, $E(N, Z)$, as a function of the proton number (Z) and neutron number (N) or atomic mass number ($A = N + Z$) is very well described by the celebrated empirical mass formula (see, e.g., [1]):

$$E(N, Z) = E_V + E_S + E_C + E_A + E_W + E_P + E_{\text{SHELL}}. \tag{1}$$

The various terms have a clear physical meaning. The volume term, $E_V = -a_V A$, describes the constant binding energy of a nucleon in saturated nuclear matter. The surface energy, $E_S = a_S A^{2/3}$, accounts for the lack of neighbors in the surface. The term, $E_C = a_C Z^2/A^{1/3}$, is the electrostatic Coulomb energy. The (a-)symmetry energy, $E_A = a_A (N - Z)^2/A$, consists of two approximately equal contributions. The "kinetic" part accounts for the Pauli principle, which requires the nucleons to occupy higher single-particle levels with increasing asymmetry $|N - Z|$. The "interaction" part originates from the difference between the proton-proton, neutron-neutron, and proton-neutron interactions. The pairing energy (E_P) describes the energy gain by forming pairs of protons or neutrons. The shell energy (E_{SHELL}) is a manifestation of the level bunching around the Fermi level. The term, $E_W = a_W |N - Z|/A$, is called the Wigner energy, because Wigner [2] gave a first interpretation in terms of his supermultiplet theory. However, its physical origin was the subject of a long debate, which was recently reviewed by [3]. Modern mean-field approaches reproduce the ground-state energies very well, except the Wigner energy, which has to be added as an *ad hoc* phenomenological term (see, e.g., [4]). This means that the physics behind the Wigner energy is not taken into account by present mean-field theories.

In this letter we demonstrate that the Wigner energy is obtained, without introducing any new parameters, by including the isovector proton-neutron pair correlations determined by numerical diagonalization of an isorotational invariant pairing Hamiltonian.

Experimentally, the coefficients a_A and a_W are not very different. The ground-state isospin (T) of most nuclei is equal to their isospin projection ($T_z = \frac{N-Z}{2}$). The sum of the symmetry and Wigner energies is approximately proportional to $T(T +$

1). The T dependence is suggestive, because the isospin operators obey the same SU_2 algebra as the angular momentum operators. Spontaneous breaking of the rotational symmetry by the deformed mean field leads to the appearance of rotational bands. The energies of the rotational levels are proportional to $I(I + 1)$, with I being the angular momentum. The analogy between nuclear spin and isospin led Frauendorf and Sheikh [5,6] to suggest that the $T(T + 1)$ dependence of the ground-state energy is a manifestation of an isorotational band.

The band appears because the isovector pair field, which is a vector, spontaneously breaks rotational symmetry in isospace. Glowacz, Satula, and Wyss discussed the analogy of the cranking model in isospace [7,8]. In the limit of strong symmetry breaking, simply the isorotational energy $T(T + 1)/2\Theta$ is added to the intrinsic energy of the symmetry breaking mean field, the orientation of which can be taken such that the proton-neutron pair field is zero [5,6]. Afanasjev *et al.* [9–11] successfully used this simple limit to interpret the excitation spectra of nuclei with $N \approx Z$.

In a series of papers, Jänecke and coworkers [12] and earlier work cited therein [13,14], demonstrated that the global $N - Z$ dependence of the binding energies, including the Wigner term and the inversion of the $T = 0$ and $T = 1$ states in odd-odd $N = Z$ nuclei with $A > 40$, can be well understood in terms of the competition between the familiar pair gap Δ and a symmetry energy term of the form $T(T + 1)$.

Applying the mean field and random phase approximation to an isorotational invariant isovector pairing interaction, Neergård has reproduced the experimental observation $a_A \approx a_W$ [3,15,16]. The virtue of such an approach is that the Wigner energy appears without introducing any new parameter, because the strength of the proton-neutron pair correlation is fixed by the isorotational invariance of the isovector pairing Hamiltonian.

However, this approach only works well when sufficiently far from the critical coupling strength for the appearance of the isovector pair field. This cannot be expected to be always the case in the medium mass nuclides, where the Wigner energy plays an important role. To avoid these problems, in this paper we treat the pair correlation into account by numerically diagonalizing the isovector pair Hamiltonian within a configuration space spanned by seven single-particle levels nearest the Fermi

surface. We demonstrate that the detailed values of the Wigner energy depend on the level spacing at the Fermi surface, and that its variations with particle number can be reproduced using single-particle energies of the Nilsson potential. In addition, we test the robustness of the results with respect to the presence of isoscalar pair correlations.

Section II presents the separation of the Coulomb energy from experimental total binding energies and describes how the experimental values of the Wigner energy, symmetry energy, and even-even odd-odd pair gaps are derived. The model is presented in Sec. III and its parameters are fixed in Sec. IV. Section V contains the results for a pure isovector pair interaction. The consequences of an additional isoscalar pair interaction are discussed in Sec. VI. The consequences of using a small number of single-particle states when calculating pair correlations are discussed in Sec. VII.

II. EXTRACTION OF THE RELEVANT EXPERIMENTAL DATA

A. Coulomb energy

As a starting point we assume that the isospin mixing caused by the Coulomb interaction can be neglected. Reference [17] estimated the admixture of components with $T > T_z$ to the ground state to be of the order of 0.9% for $A \sim 70$. With this assumption, the Coulomb energy can be separated from the energy caused by the strong interaction. Following [12] we subtract the Coulomb energy from the experimental energies and compare the resulting energies with our model. Because the mass tables have been revised, meanwhile, we repeated the extraction of the strong interaction part of the binding energies.

The expression for the Coulomb energy given in Ref. [18] is adopted:

$$E_C = \frac{3}{5}\frac{q^2}{4\pi\epsilon_0 r_0}\frac{Z^2}{A^{1/3}}\left(1 - \frac{5}{6}\left(\frac{d\pi}{r_0 A^{1/3}}\right)^2 - 5\left(\frac{3}{16\pi Z}\right)^{2/3}\right),$$
(2)

where the two unknowns are the equivalent radius (r_0) and diffuseness (d).

This expression for Coulomb energy begins with the approximation that the nucleus is a homogeneously charged sphere. The first correction takes into account diffuseness of the nuclear surface. The second is the exchange correction which is necessary because protons obey the Pauli principle and wave functions cannot completely overlap (e.g., [19]).

Using the finite difference approximation evaluated at an average value of proton number ($\bar{Z}$), a more useful expression involving energy differences results:

$$\left.\frac{\partial E_C}{\partial Z}\right|_{Z=\bar{Z}} \approx \left.\frac{\Delta E_C}{\Delta Z}\right|_{Z=\bar{Z}}$$
$$= \frac{6}{5}\frac{q^2}{4\pi\epsilon_0 r_0}\frac{\bar{Z}}{A^{1/3}}\left(1 - \frac{5}{6}\left(\frac{d\pi}{r_0 A^{1/3}}\right)^2 - \frac{10}{3}\left(\frac{3}{16\pi\bar{Z}}\right)^{2/3}\right).$$
(3)

For mirror nuclei, $\bar{Z}/A = 1/2$ the two corrections, which depend on powers of $\bar{Z}/A$ become constants. Experimental
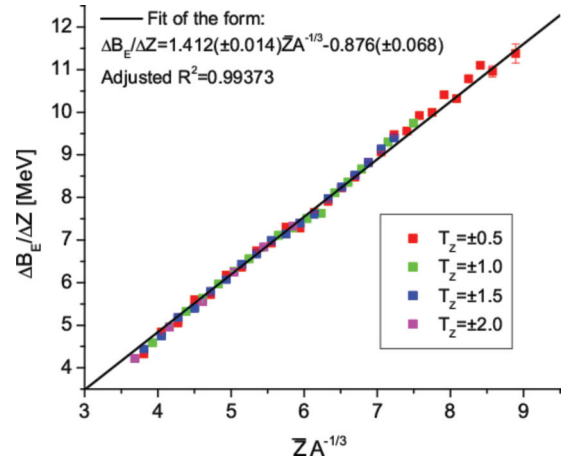

FIG. 1. (Color online) Linear fit to experimental binding energy differences of mirror nuclei plotted as a function of $\bar{Z}A^{-1/3}$. The color indicates the isospin of the pair of mirror nuclei used.

binding energies for 69 pairs of mirror nuclei in the region $20 \leqslant A \leqslant 100$ are found in the 2012 Atomic Mass Evaluation (AME) [20]. The fit shown in Fig. 1 determines the two unknowns $r_0 = 1.224$ fm and $d = 0.281$ fm. The diffuseness is not consistent with other estimates because other higher order contributions to the Coulomb energy have been combined [18].

The atomic binding energies used in these calculations also contain a small contribution accounting for the binding of the electrons, which was found to be [21]

$$B_{el}(Z) = 14.4381Z^{2.39} + 1.555 \times 10^{-6}Z^{5.35}\text{ eV.}$$
(4)

Each of the comparisons discussed here involve differences between neighboring nuclei. For these differences the term contributes at most about 15 keV. Nonetheless these contributions are taken into account.

Applying the finite difference approximation to the pairs of mirror nuclei reduces Eq. (2) to two terms because $\bar{Z} = A/2$. It can be fit with a root-mean-squared deviation of 104 keV as shown in Fig. 1, with

$$\frac{\Delta E_C}{\Delta Z} = 0.706(\pm0.007)A^{2/3} - 0.876(\pm0.068)[\text{MeV}],$$
(5)

which is comparable to previous fits (cf., e.g., [22–24]). The A-independent correction is determined by the radius, which was taken from fit of the slope. The remaining term depends on the diffuseness, which was adjusted. The resulting expression for the differences of the Coulomb energy, in steps of $\Delta Z = 2$, within an isobaric chain was used to calculate the differences between the strong interaction energies:

$$E_S(Z+1, A) - E_S(Z-1, A)$$
$$= E_{\text{Exp}}(Z+1, A) - E_{\text{Exp}}(Z-1, A)$$
$$- 2\left[1.412(\pm0.014)\frac{Z}{A^{1/3}} - 0.610(\pm0.048)\frac{Z}{A}\right.$$
$$\left. - 0.719(\pm0.007)\frac{Z^{1/3}}{A^{1/3}}\right][\text{MeV}],$$
(6)

which are needed in the expressions given in the next section.

The uncertainties of our fit are given in parentheses. They are propagated together with the quoted errors of the experimental binding energies to estimate the total error of the "experimental" quantities shown in the following figures.

B. Experimental isorotational bands

In accordance with the concept of isorotational bands, we write the energy of an isobaric chain, with constant A, in the form,

$$E(N, Z) = E_{\text{int}} + \frac{T(T + X)}{2\Theta}, \quad T = |T_z|, \quad (7)$$

where E_{int} is the energy of the intrinsic ($N = Z$) configuration. As discussed in [5,6], the Bardeen-Cooper-Schrieffer (BCS) ground state without proton-neutron pairs is a legitimate intrinsic state. It is a mixture of only even N and Z, which implies that T_z must be even if $A/2$ is even or T_z must be odd if $A/2$ is odd. Hence, the ground-state isorotational bands of even-even nuclei are composed of even values of $T = T_z$ if $A/2$ is even and odd values of $T = T_z$ if $A/2$ is odd.

The term $1/2\Theta$ is a combination of the coefficient a_S of the symmetry energy and a contribution from the shell energy $E_{\text{SHELL}}(Z, N)$, which depends on T_z. Likewise, X/Θ is a combination related to the coefficient a_W of the Wigner energy, which also contains a contribution from E_{SHELL}. We introduce the experimental isorotational frequency,

$$\omega(T + 1) = \frac{E(T + 2) - E(T)}{2} = \frac{T + 1 + X}{\Theta}. \quad (8)$$

The slope and intercept with the ω axis determine $1/\Theta$ and X. We take the experimental ground-state energies of the three nuclei with $T_z = 0, 2, 4$ if $A/2$ is even and with $T_z = 1, 3, 5$ if $A/2$ is odd and calculate two points of $\omega(T)$ be means of Eq. (8). Note that this is just a recombination of the experimental ground-state energies, which aims at exposing the Wigner energy. The explicit expressions for the experimental X are

$$X_E(A) = \left(\frac{6E_S(T_z = 0) - 8E_S(T_z = 2) + 2E_S(T_z = 4)}{-E_S(T_z = 0) + 2E_S(T_z = 2) - E_S(T_z = 4)} \right), \quad (9)$$

for even values of T_z and

$$X_O(A) = \left(\frac{8E_S(T_z = 1) - 12E_S(T_z = 3) + 4E_S(T_z = 5)}{-E_S(T_z = 1) + 2E_S(T_z = 3) - E_S(T_z = 5)} \right), \quad (10)$$

for odd T_z.

Figure 2 shows the experimental values of X, where the experimental binding energies are taken from the most recent mass evaluation from [20]. The small error bars for the lower mass region are primarily caused by the uncertainty in the spherical Coulomb energy fit. The large error bars in the $A > 80$ region are mainly caused by the error in binding energy of the nucleus nearest to or at $N = Z$.

A first determination of X based on the 2003 AME [25] generally reproduced the features described by Jänecke et al. including an apparent shift from $X \approx 1$ to $X \approx 4$ for $A > 80$. However, one new feature occurred near $A = 92$ where $X \approx 2$.
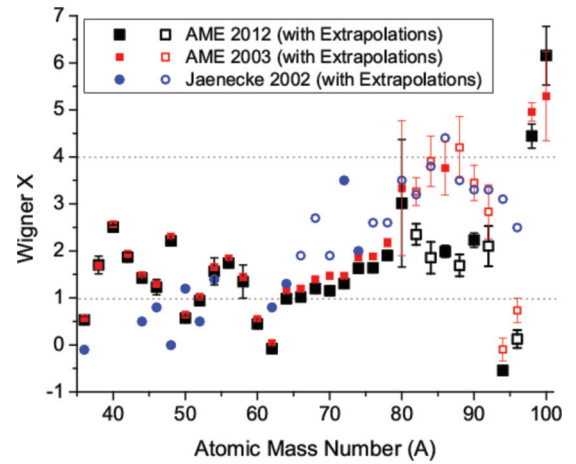

FIG. 2. (Color online) The experimental Wigner X, derived from (9) and (10). The isobaric chains were evaluated using experimental data from [25] and [20] with the Coulomb contributions removed. The X values from Jänecke et al. have been included from a comparable figure in [13]. Open symbols indicate values with at least one binding energy from an extrapolation. If not visible, the error bars are smaller than the size of the symbols.

A new observation is that as A approaches a doubly magic nucleus, the value of X appears to decrease then increase.

Jänecke suggested that the $A \approx 80$ region, the large values of X might be caused in part by the substantial uncertainties in the masses used [13]. This speculation appeared to be in agreement with the reevaluation of X based on the 2012 AME [20], upon which this paper is based. There are several changes in the $A = 80 - 90$ region, which come from a combination of new mass measurements, specifically for (^{86}Mo and ^{90}Ru) and new extrapolations (^{82}Zr, ^{84}Mo, ^{88}Ru, and ^{92}Pd) [20]. The systematic nature of the reduction of the value of X in the $A = 82 - 92$ chains is a result of the fact that the binding energy of the $T_Z = 0, 1$ nuclides has decreased by approximately 0.5–1 MeV [20]. The lowering of these points leads to smaller values of X.

Further changes of the earlier evaluations result from new masses at $T_z = 5$ (^{22}C, ^{26}O, ^{34}Mg, and ^{38}Si) and $N = Z$ (^{100}Sn) which have changed by a few hundred keV or more. Elsewhere the difference in X between AME 2003 and 2012, results from the different Coulomb fits for the two data sets. The results based on the 2012 masses have an average value of $X = 1.64$ for $24 \leqslant A \leqslant 100$.

III. THE MODEL

A monopole isovector pairing Hamiltonian is used to describe the pair correlated ground state,

$$H_V = \sum_k \epsilon_k \hat{N}_k - G_V \sum_{kk', \tau} \hat{P}^+_{k, \tau} \hat{P}_{k', \tau} + C\vec{T} \cdot \vec{T}, \quad (11)$$

$$\hat{N}_k = \hat{p}^+_k \hat{p}_k + \hat{p}^+_{\bar{k}} \hat{p}_{\bar{k}} + \hat{n}^+_k \hat{n}_k + \hat{n}^+_{\bar{k}} \hat{n}_{\bar{k}}, \quad (12)$$

$$\hat{P}^+_{k,0} = \frac{1}{\sqrt{2}} (\hat{n}^+_k \hat{p}^+_{\bar{k}} + \hat{p}^+_k \hat{n}^+_{\bar{k}}), \quad (13)$$

$$\hat{P}^+_{k,-1} = \hat{p}^+_k \hat{p}^+_{\bar{k}}, \quad \text{and} \quad \hat{P}^+_{k,1} = \hat{n}^+_k \hat{n}^+_{\bar{k}}, \quad (14)$$

where $\hat{p}_k^+$ and $\hat{n}_k^+$ create a proton and a neutron, respectively, on the level k, and $\bar{k}$ denotes the time reversed state of k. Identical single-particle energies ϵ are used for protons and neutrons, which are derived from the Nilsson potential as described in Sec. IV. This Hamiltonian is invariant under rotations in isospace, i.e., it conserves isospin.

The many-body problem is solved via matrix diagonalization. The space comprises the single-particle configurations that are generated from the lowest configuration with $T = T_z$ by multiple application of the interaction. The subsequent applications are carried out by a computer code, which stops when no new configurations are generated. As the dimension of the configuration space grows quickly with the number of active single-particle levels, it is assumed that the pair correlations are restricted to the configurations within the set of seven levels centered about Fermi level $\epsilon_{k=N}$ of the $N = Z$ nuclide within the considered isobaric chain. All levels $\epsilon_{k<N-3}$ are assumed to be occupied and all levels $\epsilon_{k>N+3}$ to be free. Because the matrix is constructed by successive application of the isospin conserving pairing interaction onto the uncorrelated ground state, the configuration space contains only states with $T = T_z$. The isobaric chains $T_z = 0, 2, 4$ are studied if $A/2$ is even or $T_z = 1, 3, 5$ if $A/2$ is odd. The respective dimensions are 3647, 1890, 210 or 3647, 1001, 70. In the case of odd-odd $N = Z$ nuclei, the lowest $T = 1$ energy is equal to the energy of the $T = T_z = 1$ isobar. As a test of the code, we also generated the configuration matrix for the odd-odd nucleus by starting from the configuration with the odd proton-neutron pair on the Fermi level in the $T = 1$ state and diagonalized it. As it has to be, the two energies agreed. The lowest $T = 0$ state in odd-odd $N = Z$ nuclei was obtained by generating the configuration matrix starting from the configuration with the odd proton-neutron pair on the Fermi level in the $T = 0$ state and diagonalizing it. This is equivalent with blocking the Fermi level from the correlations because the isovector interaction cannot scatter the isoscalar pair onto other levels nor scatter isovector pairs onto the Fermi level.

The diagonalization was carried out disregarding the levels $\epsilon_{k<N-3}$ and $\epsilon_{k>N+3}$. To the energies resulting from the diagonalization the sum of the single-particle energies for all occupied proton and neutron levels below the seven-level window was added. As discussed in the next section, this ensures that the shell correction to the binding energies is properly taken into account.

As suggested by Neergård [3], the term $C\vec{T} \cdot \vec{T}$ is a simple way to take into account the isospin dependence of the single-particle levels. The relation between the isospin dependence of the nuclear potential and the "interaction" part of the symmetry energy was discussed by Bohr and Mottelson [19]. It needs to be added, because we carry out the diagonalization of the pairing Hamiltonian for a fixed set of single-particle levels along an isobaric chain. This means that only the "kinetic" part of the symmetry energy is taken into account. The difference between the proton and neutron nuclear potentials generates an orientation in isospace. Hence it must be included in the isorotational energy. It appears in a natural way if one carries out "isocranking" about the z axis, which is just the standard procedure of fixing $\langle N \rangle$ and $\langle Z \rangle$ in self-consistent Hartree-Fock-Bogoliubov calculations.

IV. DETERMINATION OF THE MODEL PARAMETERS

The single-particle energies are calculated by means of the micro-macro method using a Nilsson Hamiltonian as described in Ref. [26]. For each nucleus the equilibrium deformation was calculated. In these calculations BCS pairing was used with $\Delta_Z = 13.4[\text{MeV}]/A^{1/2}$ and $\Delta_N = 12.8[\text{MeV}]/A^{1/2}$ as suggested in [27]. Reference [28] discusses this procedure of determining the equilibrium deformation called AutoTAC in more detail. The resulting deformations are comparable with those from Ref. [29]. The single-particle energies used in the diagonalization of the pairing Hamiltonian are taken as the average of the proton and neutron energies calculated by the Nilsson model at equilibrium deformation.

The use of the averaged energies is justified as follows. The premise of our model is that isospin is conserved, i.e., the relative energies of the proton levels and the relative energies of the neutron levels must be the same. That is, the proton levels can only be shifted by a constant energy relative to the neutron levels. The experimental studies of nuclei belonging to an isospin multiplet shows that the relative energies of exited states agree with each other within about 100 keV. These Coulomb shifts are not properly accounted for by the differences between the proton and neutron single-particle energies of the Nilsson model (or other potentials). For this reason, we chose to take the average. An overall shift of the proton levels by a constant energy results in a constant shift of the average single-particle energy, which does not matter, because we only consider energy differences.

The bunching of the single-particle levels generates the shell effects in the binding energies. In the framework of the micro-macro method the shell correction is the sum of the single-particle energies of all occupied levels minus the Strutinsky average of this sum. The latter term is a smooth function of N and Z. For the energy differences investigated in this paper, it either (nearly) cancels out or can be considered being incorporated in the $CT(T + 1)$ term of the model (cf. Sec. V A). Thus adding the sum of the single-particle energies below the seven-level window will correctly reproduce the shell correction to the energy differences.

The model contains two parameters, strength of the isovector pair interaction G_V, and the parameter C of the "symmetry" interaction, which have been determined by simultaneously fitting the even-even odd-odd mass differences and the energy difference between the $T = 0$ and $T = 1$ states in the odd-odd nuclei.

As well known from BCS theory, the value of G_V has to be adjusted to the number of levels taken into account. We adopt the standard procedure to reproduce the experimental values of the even-odd mass differences, which scatter around the smooth dependence on the atomic mass number of

$$\Delta \approx \frac{12}{A^{1/2}}[\text{MeV}], \tag{15}$$

for both protons and neutrons (e.g., [27], [18]). Because our computer code can only handle even-A nuclei, we use the mass differences between the even-even and odd-odd $N = Z$ nuclides derived by means of the three-point formula:

$$2\Delta(N, Z) = \frac{B_E(N - 1, Z - 1) - 2B_E(N, Z) + B_E(N + 1, Z + 1)}{2},$$

(16)

to determine $G_V(A)$. Coulomb, surface, volume, and symmetry terms in the binding energy approximately cancel out using this difference. The mass differences have a global dependence on A roughly twice that given by Eq. (15) [30]. Equation (16) was evaluated using the binding energies of the even $N = Z$ nuclides and the binding energies of the $T = 0$ states of the odd $N = Z$ nuclides. The following fit was adopted:

$$G_V = \frac{13.9}{A^{3/4}}[\text{MeV}].$$

(17)

The values based on experimental binding energies were compared with the ones obtained from calculated energies using $G_V(A)$ as given by Eq. (17) and Nilsson levels corresponding to AutoTAC equilibrium deformation. In calculating the odd-odd nuclei, the fourth (middle) level was blocked, because the $T = 0$ states have two quasiparticle character with respect to isovector pair correlations. The blocking procedure is described in detail in [31]. In essence, the blocked level was disregarded in constructing the matrix and twice its energy was added after the diagonalization. Figure 3 compares the experimental with the calculated values. Overall, there is good agreement. The deviations are likely a result of inaccuracies of the Nilsson levels. The deformations resulting from the AutoTAC calculation are often substantially smaller than those determined experimentally using $B(E2)$ values.

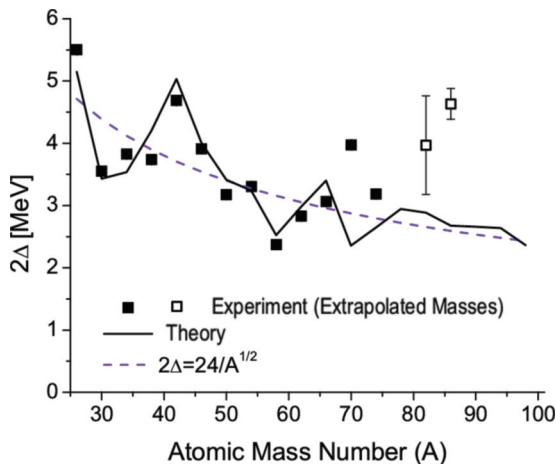The competition of the first $T = 0$ and first $T = 1$ states of odd-odd $N = Z$ was then used to fix the parameter C.

FIG. 3. (Color online) The even-even odd-odd mass difference 2Δ obtained from (16) using modified energies from [20] with the Coulomb energy removed. The solid line shows the calculations. The purple dashed line is the global fit of $2\Delta = 24A^{-1/2}[\text{MeV}]$. If not visible, the error bars are smaller than the size of the symbols.
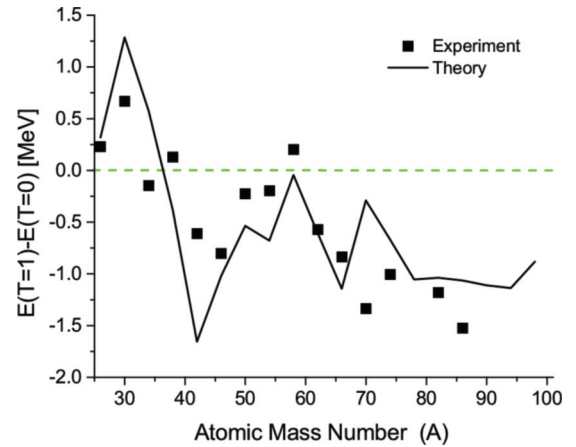

FIG. 4. (Color online) Energy difference of the first $T = 1$ from the first $T = 0$ states in odd-odd $N = Z$ nuclei. The solid line shows the calculations. Experimental data from NNDC [32]. The green dashed line indicates where inversion occurs.

The theoretical energy difference $E(T = 1) - E(T = 0)$ was obtained by a seven-level calculation for the $T = 1$ state and for the $T = 0$ state by the "blocked" calculation described in the preceding paragraph. Without the symmetry interaction term, the fully correlated $T = 1$ state lies at least 2Δ below the blocked $T = 0$ state. However, the inclusion of the symmetry interaction term ($2C$ is added to the $T = 1$ state) results in comparable energies for the two states. With increasing A, the levels switch order, which is seen experimentally [32] (as discussed in [14]).

Requiring the smooth $1/A$ dependence of the symmetry energy, the fit of the calculated differences $E(T = 1) - E(T = 0)$ to the experimental ones gave

$$C = \frac{58.9}{A}[\text{MeV}].$$

(18)

As already discussed, odd-odd $N = Z$ nuclei with $A > 40$ have a ground state that has $T = 1 > T_z = 0$. The inversion of the isospin order was explained by Refs. [23,30]. The $T = 0$ state in the odd-odd nucleus is lifted relative to the $T = 0$ ground state of the even-even neighbors, by the two quasiparticle excitation energy 2Δ. The $T = 1$ state is lifted by the isorotational energy $1/\Theta$, which is somewhat smaller than 2Δ.

Figure 4 shows that calculations well reproduce energy difference between the lowest $T = 1$ and $T = 0$ states, which measures to relative strength of the isovector pair correlation and the isorotational energies. There are large fluctuations in the theoretical calculations caused by the uneven level spacings, which are roughly reproduced. The deviations are of the same order as the ones of 2Δ and have the same origin.

The coefficient of the symmetry energy in the liquid drop model $4a_A = 1/2\theta_{\text{LD}} = 100$ MeV/A. The value of $C = 58.9$ MeV/A is consistent with the general estimates [19] that the interaction part of the symmetry energy amounts to about 50% of its total value.
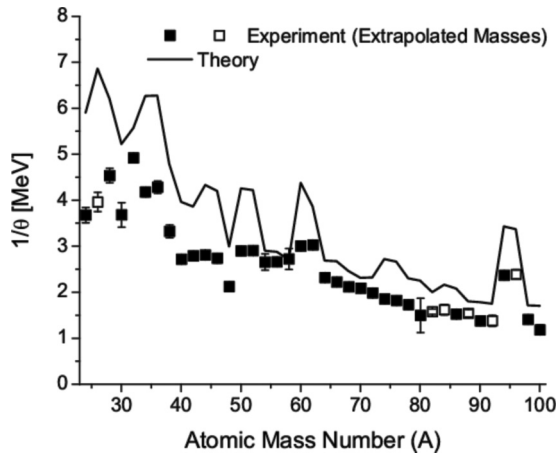
FIG. 5. Slope of the isobar energies obtained from (19) using modified energies from [20] with the Coulomb energy removed. If not visible, the error bars are smaller than the size of the symbols. The solid line shows the calculations.

V. RESULTS—PURE ISOVECTOR PAIRING

A. The isorotational moment of inertia

Combining the energy differences as

$$\frac{1}{\theta} = \frac{E_S(T_z = 0, 1) - 2E_S(T_z = 2, 3) + E_S(T_z = 4, 5)}{4},$$

(19)

the local slope for both the even and odd chains of T_z was calculated. It has the meaning of the inverse moment of inertia of the isorotational sequence. Figure 5 displays a comparison between experiment and theoretical calculation of the slope.

The calculated values of $1/\theta$ are systematically somewhat larger than the experimental ones. We believe that this reflects a fringe effect of our small single-particle space. The number of configurations decreases from 3647 to 1001 and finally to 70 for $T = 0, 2, 4$, respectively. This results in a decrease of the pair correlation energy, which is reflected by an increase of $1/\theta$. The consequences of the small number of single-particle levels will be discussed in more detail in Sec. VII.

B. The Wigner X

Figure 6 demonstrates that the calculations reproduce well the observed values of X, both the average, which is somewhat larger than 1, and the pronounced fluctuations. As seen in Fig. 2, the X values derived from the most recent mass tables agree much better with the calculation than the ones derived by Jänecke *et al.* [12] from the 2002 mass tabulations. In the region $A \approx 58$, the X values based on the AutoTAC deformations overestimate the amplitude of the oscillation. As shown in the schematic calculations discussed below, the amplitude of the fluctuations is largest for strong bunching of levels that occurs near a doubly magic nucleus. The static AutoTAC deformations in this region are mostly zero. The degeneracy of the spherical levels will be partially lifted by shape vibrations, which will damp the fluctuations.
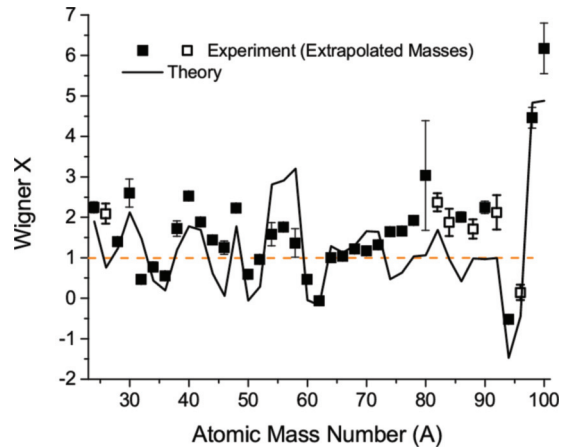

FIG. 6. (Color online) The Wigner X obtained from (9) and (10) using modified energies from [20] with the Coulomb energy removed. If not visible, the error bars are smaller than the size of the symbols. Solid line shows the calculations. The orange dashed line indicates $X = 1$.

There is a tendency that the calculations underestimate X for $74 \leqslant A \leqslant 92$. There are two possible justifications for the discrepancies seen in this region. The experimental uncertainties are large in this mass region and several binding energies are extrapolated. Additionally, the AutoTAC deformations are moderate and fairly constant, which results in X values close to one. Experimental yrast energies of these nuclei indicate a change from more vibrational to more rotational behavior as T_z increases, which should be caused by an increasing deformation.

The fluctuations of the calculated quantities reflect the irregular level spacings. Figure 7 illustrates the effects on the observed X caused by changes in level density. The system with even level spacing is intended to simulate well-deformed nuclei. The gaps in the spectrum simulate the bunching of
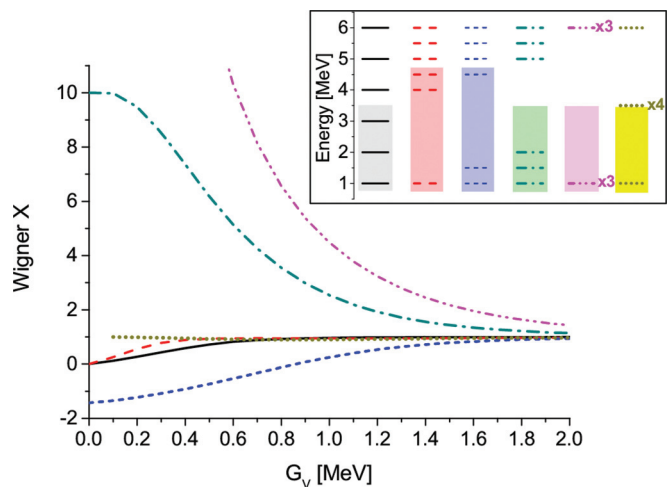

FIG. 7. (Color online) Wigner X for various level arrangements. For $G = 0$ and $T_z = 0$, the levels 1,2,3 are occupied and 4,5,6 empty. Configurations with larger T_z are generated by removing proton pairs and placing neutron pairs according to the Pauli principle. The average spacing of the energy levels is 1 MeV. Note $C = 0$.
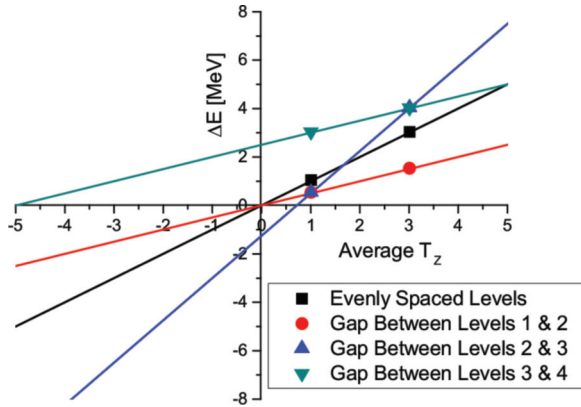
FIG. 8. (Color online) Linear fits corresponding to energy differences for the levels shown in Fig. 7 without pair correlations. The slope and intercept are related to $1/\theta$ and X, respectively.

levels for nuclei with a nearly spherical shape. In the strong pairing limit, the isorotational band structure is restored and $X = 1$. To approach the limit, the pair field Δ must be several times the average level spacing, such that local fluctuations of the latter are averaged. The interaction strength $G_V < 1.5$ MeV is not strong enough to averaging out fluctuations of X about 1. The same holds for the fluctuations of 2Δ and $1/\theta$.

The deviations from the smooth trends can be understood by considering the limit $G_V = 0$, when the energy is simply the sum of the energies of the occupied levels. Figure 8 illustrates that the various level distributions generate different values of X and $1/\theta$ for $G_V = 0$, which are still apparent in the calculations with realistic G_V values. In particular, the strong up-down of X, which is seen experimentally around $A = 40$, 56 and possibly $A = 100$, is caused by moving through the respective shell gaps.

VI. INFLUENCE OF THE ISOSCALAR INTERACTION

We have also studied the possible influence of isoscalar proton-neutron pair correlation on the Wigner X by supplementing the Hamiltonian (11) with the term,

$$H_{V+S} = H_V - G_S \sum_{kk'} \hat{S}_k^+ \hat{S}_{k'}, \hat{S}_k^+ = \frac{1}{\sqrt{2}}(\hat{n}_k^+ \hat{p}_{\bar{k}}^+ - \hat{p}_k^+ \hat{n}_{\bar{k}}^+),$$

(20)

where G_S is the isoscalar interaction strength. The isoscalar pair operators create proton-neutron pairs in states with opposite projection of the angular momentum. The rational for using such an interaction is that the strong spin-orbit coupling generates this type of degenerate time-reversed states, which are expected to be correlated. This was used by Chasman before [33], and the inclusion of this type of interaction into our model is straightforward, however, it generates many more configurations. For example, a six-level calculation using the pure isovector Hamiltonian (11) with six protons and six neutrons has 1001 configurations, while including the isoscalar contributions results in 1992 configurations. As a result, only six levels could be used for the isovector plus

isoscalar calculations. The dimensions are 1992, 825, 66 for $T = 0, 2, 4$, respectively.

The calculations were carried out for fixed ratios of $G_S/G_V = [0, \frac{1}{8}, \frac{1}{4}, \frac{1}{2}, 1, 2, 4, 8]$, using the six Nilsson levels nearest the Fermi surface, which were determined as described above. The parameters $G_V(A)$ and $C(A)$ were determined as before by fitting the experimental values of 2Δ and $E(T = 1) - E(T = 0)$. The results are summarized in Fig. 9. Note that the $G_S = 0$ calculation differs from the previously discussed calculations because the number of levels has changed. This reduction of the number of levels from seven to six requires a renormalization of G_V, which increased by about 5%. The $C(A)$ values are also renormalized and decreased by about 4%. The actual fit values used are included in the figure. As a whole, the results only insignificantly change within the displayed range of the ratio between the interactions. For $G_S > G_V/2$ it was not possible to simultaneously fit 2Δ and $E(T = 1) - E(T = 0)$.

Figure 10 shows schematic calculations of the four quantities of interest for six equidistant levels. The value of $C = 1$ MeV was chosen with the intention to simulate nuclei near $A = 60$. As expected, for G_S substantially larger than G_V, the even-even odd-odd mass differences approach zero and become slightly negative. This is the signature of an isoscalar pair condensate, where even-even and odd-odd $N = Z$ nuclides merge into a pair-rotational band [6,34]. To remain within the experimental band of 2Δ, the isovector correlations must prevail. That is, the stripe of experimental values of 2Δ lies always below the diagonal. Note that the value of 2Δ does not depend on C, because it involves a comparison of $T = 0$ states only.

Comparing the four panels in Fig. 10, one notices that the quantities $E(T = 1) - E(T = 0)$, X and $1/\theta$ do not change much along a contour of constant 2Δ, as long as one stays within the band of experimental values delineated by the dashed lines and the interval $0 < G_S/G_V < 0.5$, which is the range of ratios shown in Fig. 9. This helps to explain why the experimental data could be equally well reproduced within this range. Hence, the coexistence of a moderate amount of isoscalar pair correlations is consistent with the data, which, however, does not provide evidence for its existence. Large-scale shell-model calculations with realistic effective interactions find moderate isoscalar pair correlations coexisting with strong isovector correlations [35,36].

Our results do not concur with Refs. [37–40] which relate the Wigner energy to the presence of isoscalar proton-neutron pair correlations. However, they are consistent with the findings of Ref. [35], which pointed out that although the Wigner term is related to the $T = 0$ part of the residual interaction in shell-model calculations this does not necessarily imply that it is generated by proton-neutron pair correlations.

VII. FRINGE EFFECTS

The small number of single-particle levels among which the pair correlations are allowed to act causes artifacts that will be quantified now. As discussed in Sec. V A, the number of configurations available for pair correlations strongly decreases
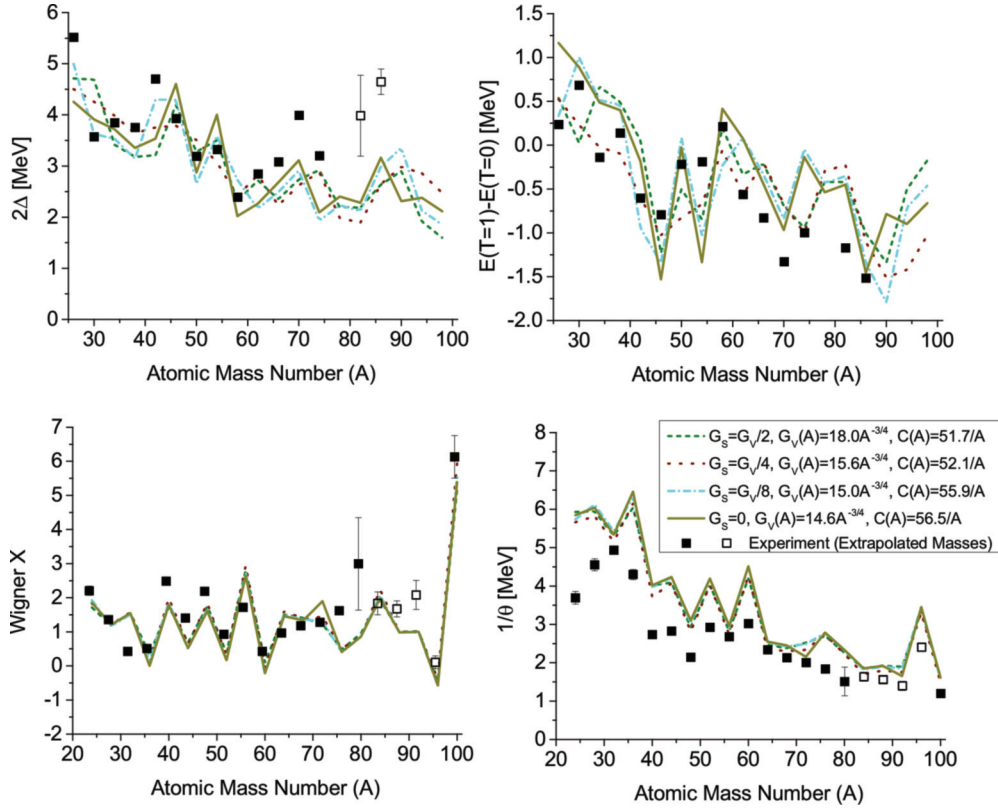
FIG. 9. (Color online) 2Δ, $E(T = 1) - E(T = 0)$, X_E, and $\frac{1}{\theta}$, using the fixed interaction strengths ratios, and listed as $G_V(A)$ and $C(A)$ (both in units of MeV), compared to experiment. If not visible, the error bars are smaller than the size of the symbols.

with T (by a factor of 50) when the Fermi level approaches the upper single-particle level, because the combinatorial possibilities are reduced. This results in an artificial reduction of the pair correlations, which we called the fringe effect. The reduction of the pair correlation energy increases $1/\theta$, which is in our view the reason why this quantity comes out systematically somewhat too large.

The fringe effect on $1/\theta$ can be estimated on the basis of Fig. 10, which shows calculations for six equidistant levels. The slope $1/\theta$ increases from 3.00 to 3.32 MeV when G_V changes from 0 to a realistic value of 1 MeV, while holding $G_S = 0$. This puts a scale on the fringe effects, because $1/\theta$ should not change with the strength of the pair correlations for a sufficiently large set of equidistant levels. Instead, it should stay equal to the value without pair correlations. More specifically, it should be $d + 2C$, with $d = 1$ MeV being the average level spacing and $C = 1$ MeV being the strength of the symmetry interaction for this case. The difference of 0.32 MeV is consistent with the systematic overestimation of $1/\theta$ in Figs. 5 and 9 around $A = 80$.

The six-level and seven-level calculations give nearly the same values of $1/\theta$. This can be seen by comparing Fig. 5 with Fig. 10. Note, in the latter, only even T chains have been evaluated. More quantitatively, the respective mean values of $1/\theta$ are 3.49 MeV and 3.47 MeV, and the respective mean square deviations are 0.90 MeV and 0.93 MeV. The contribution of the symmetry interaction to $1/\theta$ is equal to

$2C$. The fact that a smaller C in six-level calculation gives the same values of $1/\theta$ as the seven-level calculation means that the fringe effect must be larger for six than for seven levels, which is compensated by the reduction of C. For $A = 80$ the difference of $2C$ between the seven- and six-level cases is 0.06 MeV. This increase of $2C$ compensates a decrease of the fringe effect in the seven-level calculations by the same amount. This value is 20% of the 0.32-MeV estimate in the preceding paragraph.

Using approximately 60% the value for $C(A)$ would reconcile the discrepancy in $1/\theta$ between experiment and theory. However, it would result in a systematic overestimate of $E(T = 1) - E(T = 0)$. This fringe effect, which is a limitation of our few-level approach, leads us to use $E(T = 1) - E(T = 0)$ in the odd-odd $N = Z$ to adjust the C parameter nuclei, where the effect is weakest, instead of determining it from the experimental slope of the symmetry energy. The main focus of our work is the study of the Wigner X, which impacts the nuclei near $N = Z$ strongest. The studies of Refs. [12,30] demonstrated that the experimental values of $1/\theta$ and 2Δ are consistent with $E(T = 1) - E(T = 0) = 2\Delta - 1/\theta$ on average. We expect that including more single-particle levels into the beyond-mean-field description of the pair correlations will resolve the modest inconsistency. Unfortunately, direct diagonalization of the pairing Hamiltonian will not be feasible because of the combinatorial explosion of the dimensions. A shift of the single-particle window to have the same number
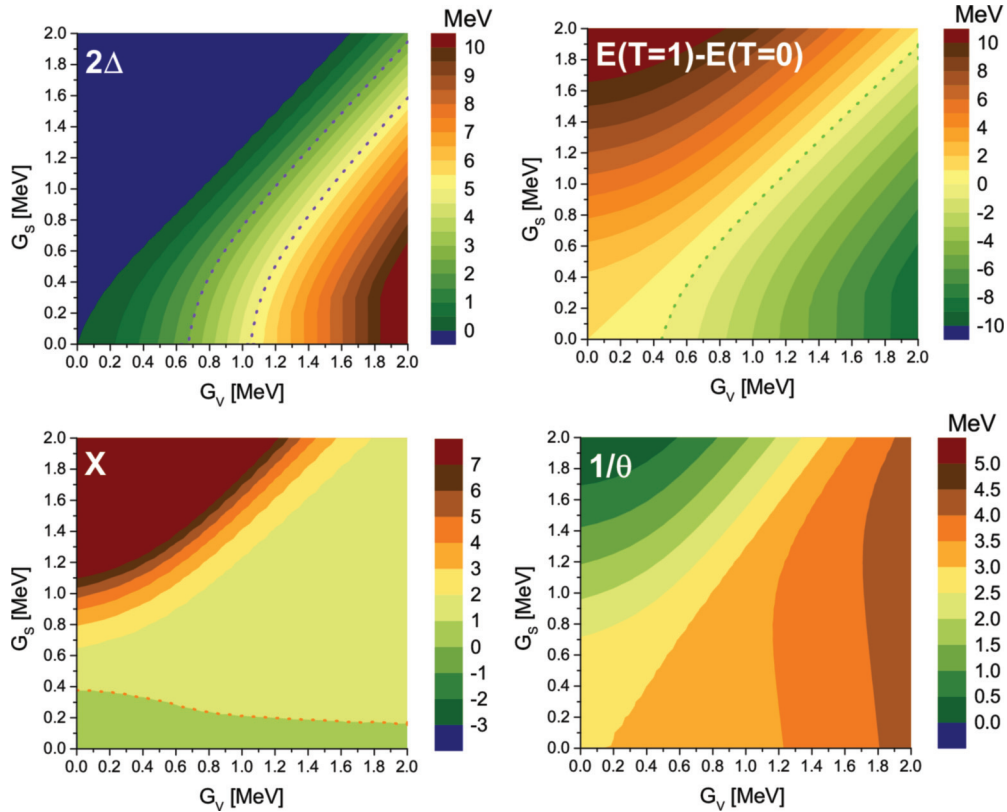
FIG. 10. (Color online) Isovector plus isoscalar calculation for equidistant levels. The dotted purple lines indicate the smoothed trends of 2Δ in Fig. 3 around $A = 20$ and $A = 100$, respectively, the dotted green line $E(T = 1) = E(T = 0)$, and the dotted orange line $X = 1$. The level spacing is 1 MeV and $C = 1$ MeV.

of levels on both sides of the Fermi level violates isospin conservation, which is a crucial ingredient. Clearly one has to employ some approximation scheme that ensures good isospin. Work along this line is on the way.

VIII. CONCLUSIONS

We have demonstrated that a model based on single-particle levels in a deformed potential, isospin conserving isovector monopole pairing, and a schematic "symmetry" interaction proportional to $\vec{T}^2$ reproduces the term linear in $|N - Z|$ in the nuclear binding energy. The pairing correlations were treated exactly by numerical diagonalization in a space of seven single-particle levels, which ensured that isospin was conserved. Isospin invariance requires the coupling constants of the proton-proton, proton-neutron, and neutron-neutron interaction to be equal.

The Wigner term appears as a result of breaking isospin invariance on the mean-field level. The deformation in isospace gives rise to an isorotational band with energies $\propto T(T + 1)$. The deformation is caused by the isovector pair field and the differences between the proton and neutron nuclear potentials to about equal parts.

The model does not introduce new parameters as compared to standard mean-field approaches. The two model parameters are the pairing strength, which is fixed by the even-even to

odd-odd mass difference, and the strength of the symmetry interaction, which is determined by the energy difference between the lowest $T = 0$ and $T = 1$ states in odd-odd $N = Z$ nuclei. Using this approach it is possible to get roughly the correct order ($T = 0$ below $T = 1$ for $A < 40$ and $T = 1$ below $T = 0$ for $A > 40$).

Merging the symmetry term and the Wigner term of the binding energy into one expression of the form $T(T + X)/2\theta$, the values of X are found to scatter around 1. The limit $X = 1$ corresponds to a regular isorotational band, which emerges if isospin is strongly broken by the pair field. Because the realistic pair field has only moderate strength the bunching of the single-particle levels, resulting from shell structure, causes strong fluctuations of the Wigner energy which are fairly well described by the model. The remaining deviations can be attributed to inaccuracies of the calculated single-particle energies.

A combination of an isorotational invariant effective interaction in the particle-hole channel with isovector pairing interaction is capable of reproducing the Wigner energy, provided the pairing correlations are treated beyond the mean-field approximation and isospin is conserved. How to accomplish this for the present standard mean-field approaches remains to be studied. In a future study we will address this question by comparing our results with approximations as, e.g., isospin projected mean-field solutions.

In addition, we investigated how including a monopole isoscalar pairing interaction would modify the results. As long as the ratio between the isoscalar and isovector coupling constants remained smaller than 0.5, the experimental values of the Wigner energy and of the $T = 0 - T = 1$ energy difference in odd-odd $N = Z$ nuclei could be equally well reproduced after a slight readjustment of the two model parameters. The results turned out to be insensitive to moderate isoscalar pair correlation of this scale and, thus, did not provide any clue about their possible presence. Ratios of the isoscalar-isovector coupling constants larger than 0.8 contradict the experimental values of the even-even odd-mass mass differences.

ACKNOWLEDGMENT

[1] W. D. Myers and W. J. Swiatecki, Annu. Rev. Nucl. Part. Sci. **32**, 309 (1982).

[2] E. Wigner, Phys. Rev. **51**, 947 (1937).

[3] K. Neergard, Phys. Rev. C **80**, 044313 (2009).

[4] S. Goriely, N. Chamel, and J. M. Pearson, Phys. Rev. C **82**, 035804 (2010).

[5] S. G. Frauendorf and J. A. Sheikh, Nucl. Phys. A **645**, 509 (1999).

[6] S. Frauendorf and J. A. Sheikh, Phys. Scr. **T88**, 162 (2000).

[7] W. Satula and R. Wyss, Phys. Rev. Lett. **86**, 4488 (2001).

[8] S. Glowacz, W. Satula, and R. Wyss, Eur. Phys. J. A **19**, 33 (2004).

[9] C. D. O'Leary, C. E. Svensson, S. G. Frauendorf, A. V. Afanasjev, D. E. Appelbe, R. A. E. Austin, G. C. Ball, J. A. Cameron, R. M. Clark, M. Cromaz, P. Fallon, D. F. Hodgson, N. S. Kelsall, A. O. Macchiavelli, I. Ragnarsson, D. Sarantites, J. C. Waddington, and R. Wadsworth, Phys. Rev. C **67**, 021301 (2003).

[10] A. V. Afanasjev and S. Frauendorf, Phys. Rev. C **71**, 064318 (2005).

[11] C. Andreoiu *et al.*, Phys. Rev. C **75**, 041301 (2007).

[12] J. O. T. W. Jänecke, Eur. Phys. J. A **25**, 79 (2005).

[13] J. Jänecke, T. W. O'Donnell, and V. I. Goldanskii, Phys. Rev. C **66**, 024327 (2002).

[14] J. Jänecke and T. O'Donnell, Phys. Lett. B **605**, 87 (2005).

[15] K. Neergard, Phys. Lett. B **537**, 287 (2002).

[16] K. Neergard, Phys. Lett. B **572**, 159 (2003).

[17] W. Satuła, J. Dobaczewski, W. Nazarewicz, and M. Rafalski, Phys. Rev. Lett. **103**, 012502 (2009).

[18] S. Nilsson and I. Ragnarsson, *Shapes and Shells in Nuclear Structure* (Cambridge University Press, Cambridge, 1995).

[19] A. Bohr and B. Mottelson, *Nuclear Structure I: Single-Particle Motion* (World Scientific, Singapore, 1999).

[20] G. Audi, M. Wang, A. Wapstra, F. Kondev, M. MacCormick, X. Xu, and B. Pfeiffer, Chinese Physics C **36**, 1287 (2012).

[21] D. Lunney, J. M. Pearson, and C. Thibault, Rev. Mod. Phys. **75**, 1021 (2003).

[22] J. Jänecke, in *Atomic Masses*, edited by R. Barber (University of Manitoba Press, Winnipeg, 1967), p. 583.

[23] P. Vogel, Nucl. Phys. A **662**, 148 (2000).

[24] A. E. L. Dieperink and P. Van Isacker, Eur. Phys. J. A **32**, 11 (2007).

[25] G. Audi, A. H. Wapstra, and C. Thibault, Nucl. Phys. A **729**, 337 (2002).

[26] S. Frauendorf, Nucl. Phys. A **677**, 115 (2000).

[27] P. Möller and J. R. Nix, Nucl. Phys. A **536**, 20 (1992).

[28] I. Bentley and S. Frauendorf, Phys. Rev. C **83**, 064322 (2011).

[29] P. Möller, J. R. Nix, W. D. Myers, and W. J. Swiatecki, At. Data Nucl. Data Tables **59**, 185 (1995).

[30] A. O. Macchiavelli, P. Fallon, R. M. Clark, M. Cromaz, M. A. Deleplanque, R. M. Diamond, G. J. Lane, I. Y. Lee, F. S. Stephens, C. E. Svensson, K. Vetter, and D. Ward, Phys. Rev. C **61**, 041303 (2000).

[31] P. Ring and P. Schunk, *The Nuclear Many Body Problem* (Springer-Verlag, New York, 1980).

[32] J. Tuli, "Evaluated nuclear structure data file", data retrieved on December 21, 2011.

[33] R. Chasman, Phys. Lett. B **524**, 81 (2002).

[34] S. Frauendorf, Rev. Mod. Phys. **73**, 463 (2001).

[35] A. Poves and G. Martinez-Pinedo, Phys. Lett. B **430**, 203 (1998).

[36] K. Langanke, D. Dean, S. Koonin, and P. Radha, Nucl. Phys. A **613**, 253 (1997).

[37] W. Satula and R. Wyss, Phys. Lett. B **393**, 1 (1997).

[38] D. Brenner, C. Wesselborg, R. Casten, D. Warner, and J.-Y. Zhang, Phys. Lett. B **243**, 1 (1990).

[39] W.-T. Chou, J.-Y. Zhang, R. Casten, and D. Brenner, Phys. Lett. B **255**, 487 (1991).

[40] W. Satula, D. Dean, J. Gary, S. Mizutori, and W. Nazarewicz, Phys. Lett. B **407**, 103 (1997).